ELSEVIER

Journal of Molecular Catalysis A: Chemical 157 (2000) 163–171

JOURNAL OF MOLECULAR CATALYSIS A: CHEMICAL

www.elsevier.com/locate/molcata

Spectroscopic investigation and catalytic activity of copper(II) phthalocyanine encapsulated in zeolite Y

Sindhu Seelan, A.K. Sinha, D. Srinivas, S. Sivasanker *

National Chemical Laboratory, Catalysis Division, Pune 411008, India

Received 9 September 1999; received in revised form 1 November 1999; accepted 23 November 1999

Abstract

Copper phthalocyanine (CuPc) encapsulated in zeolite Y was prepared by in situ ligand synthesis method by reacting Cu(II) exchanged NaY with 1,2-dicyanobenzene followed by Soxhlet extraction with several solvents. The encapsulated copper phthalocyanine, CuPcY(e) was characterized by chemical and thermal analyses, FT-IR, diffuse reflectance UV–Vis, and EPR spectroscopic techniques. The spectral studies unequivocally prove the encapsulation of CuPc in the α-cages of zeolite Y and suggest a distortion in the CuPc moiety. The encapsulated materials were more active than neat phthalocyanine in the epoxidation of styrene with tertiary butylhydroperoxide.

Keywords: Copper phthalocyanine; Zeolite Y; Spectroscopy; EPR; Encapsulation; Styrene epoxidation

1. Introduction

One of the goals of catalysis researchers in recent times has been the synthesis of inorganic mimics of enzymes such as cytochrome *P*-450. One approach has been the encapsulation of transition metal complexes inside the cages and void spaces of zeolite and zeolitic materials [1–3], the porous inorganic mantle (zeolite) providing (hopefully) the right steric requirement for the metal complexes and imposing certain restrictions (based on size and shape) to the access of the active site by the substrate molecules. Metal complexes containing salen, porphyrin, and phthalocyanine ligands, have been the typical active centers used in the many studies on the subject [4–12]. Though many porous materials have been used, the most popular ones have been zeolites X and Y possessing large α-cages ($\sim$ 12 Å diameter). Many procedures such as ligand synthesis, template synthesis, and zeolite synthesis methods have been developed for the preparation of encapsulated metal complexes [1–3].

An important aspect of these studies is proving unequivocally the encapsulation of the complexes inside the cages (or cavities) of the zeolite to reveal these 'ship-in-bottle' systems. Though this is relatively easy with salens, the problem is difficult in the case of phthalocyanines which are large in size ($>$ 12 Å diameter) and not easy to fit inside zeolitic cages, and which tend to adsorb strongly at the external surface of the crystallites. In this communica-

* Corresponding author. Fax: +91-20-5893761.
E-mail address: siva@cata.ncl.res.in (S. Sivasanker).

1381-1169/00/$ - see front matter
PII: S1381-1169(99)00432-X

tion, we present our studies on copper phthalocyanine (CuPc) encapsulated in zeolite Y proving unequivocally the encapsulation of the complex inside the α-cages. The studies also suggest a distortion of the CuPc due to encapsulation. The catalytic study of encapsulated materials in the epoxidation of styrene with tertiary butylhydroperoxide is also reported.

2. Experimental

2.1. Materials and preparation

CuPc and 1,2-dicyanobenzene (DCB) obtained from Aldrich were used as received. All the solvents were of AR grade and obtained from S.D.-Fine Chem., India. Commercial NaY (LZ-Y-52) was used.

CuPc encapsulated in zeolite Y was synthesized by ion-exchange of Cu(II) ions in NaY followed by in situ ligand synthesis using 1,2-dicyanobenzene [9–15]. CuY samples with metal loadings of 0.6 and 1.2 wt.% were prepared by ion exchanging with a dilute solution of $Cu(NO_3)_2$. CuY, thus prepared, was dried at 373 K (6 h) in an oven, degassed (8 h) at 373 K, and exposed to DCB vapours at 473 K for 24 h under N_2 atmosphere inside a glass vessel. Unreacted DCB, Pc, and other organic matters on the surface of the zeolite were removed by Soxhlet extraction with different solvents in the order: acetone (48 h) and pyridine (120 h) to remove the extractable organics, and acetonitrile (48 h), then again, acetone (24 h) to remove the residual pyridine.

Two samples, CuPcY-1(e) and CuPcY-2(e), were prepared from CuY with 1.2 and 0.6 wt.% Cu, respectively. The final product, which was greenish blue in colour, was dried at 393 K in an oven for 24 h. A small quantity of CuPcY-1(e) was also exchanged thrice with a 1 M solution of a $CaCl_2$ (20 ml/g solid; 353 K; 6 h) to remove the uncomplexed Cu ions from the sample. This sample was designated as CuPcY-1(e)-Ca.

XRD patterns (obtained on a Rigaku DIII Max instrument) of the above encapsulated materials were similar to those of the parent NaY suggesting the absence of structural damage of the zeolite during encapsulation.

A physical mixture of CuPc (10 wt.%) in NaY was also prepared (CuPcY(m)) for comparison purposes.

2.2. Physical measurements

Carbon and nitrogen analyses were carried out using a Carlo Erba Elemental Analyser (EA 1108). Thermogravimetric and differential thermal analyses (TGA/DTA) were performed on an automatic derivatograph (Setaram TG-DTA 92). A commercial adsorption unit (Omnisorp 100 CX; Coulter, USA) was used for surface area measurements. FT-IR spectra were recorded on a Nicolet 60 SXB spectrophotometer in the range 600–4000 cm^{-1}. The diffuse reflectance UV–Vis spectra (DRS) of the solid catalysts were recorded using a UV-101 PC scanning spectrophotometer. EPR spectra were recorded on a Bruker EMX spectrometer operating at X-band frequency (9.76 GHz) and 100 kHz field modulation. Calibration of microwave frequency was done using a built in frequency counter. Spectra were recorded on both solid powders and H_2SO_4 solutions. Measurements at 77 K were performed using a quartz finger type Dewar. DPPH was used as a field marker (g = 2.0036). Spectral manipulations and simulations were done using Bruker WINEPR and Simfonia software packages.

2.3. Catalytic studies

The catalytic experiments were carried out in a 50-ml double-necked round bottom flask attached to a condenser and kept in an oil bath, Styrene (4.8 mmol), acetonitrile (solvent, 5 g), and tertiary butylhydroperoxide (4.8 mmol; solution in decane, Aldrich), and the catalyst (0.050 g) were stirred using a magnetic stirrer for 24 h. The products were analysed by a gas

chromatograph (HP 5880A; FID; 50 m × 0.2 mm capillary column).

3. Results and discussion

Copper phthalocyanines exist in several crystalline modifications of which the α and β forms are well characterized. The ''neat'' CuPc (β form) was deep blue in colour, while the encapsulated materials (CuPcY(e)) were greenish-blue, and the physical mixture, CuPcY(m), was light blue in colour.

In order to probe the formation and location of macrocyclic CuPc molecules in the zeolite, experiments were conducted on the following samples:

(i) Cu(II) exchanged NaY (CuY),
(ii) ''neat'' CuPc,
(iii) encapsulated CuPc prepared as described in the Experimental section using an in situ ligand synthesis method (CuPcY-1(e) and CuPcY-2(e)),
(iv) a physical mixture of ''neat'' CuPc and NaY (CuPcY(m)), and
(v) H_2SO_4 solutions of CuPc and CuPcY-1(e).

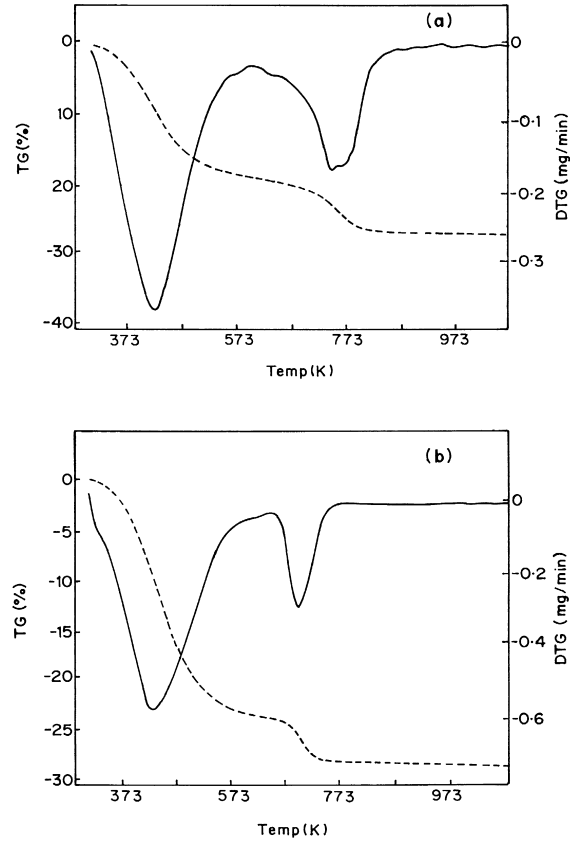

Fig. 1. TGA (----) and DTG (—) profiles of (a) CuPcY-1(e) and (b) CuPcY(m).

3.1. Chemical and thermal analyses

The chemical analyses of the samples (Table 1) reveal the presence of organic matter with an N/C ratio roughly similar to that for phthalocyanine (36 ± 1% compared to 29.2% for Pc). The total organic contents of the samples suggest the presence of 1.6 and 1.3 Pc molecules per unit cell in CuPcY-1(e) and CuPcY-2(e) synthesized from CuY samples with loadings of 1.2 and 0.6 Cu wt.%, respectively (Table 1). The thermogravimetric analyses, also reveal similar organic contents (weight loss between 473 and 873 K) in the two samples, though accurate quantification is not possible due to the additional water loss from the samples whose magnitude could itself depend on the organic content (level of encapsulation). The TGA/DTA curves of CuPcY(m) and CuPcY-1(e) are

Table 1
Physico-chemical characterization of CuPcY

Sample	Cu (wt.%)		C/N analysis (wt.%)		S^a_{BET} (m^2/g)	Pore volume (ml/g)	Molecules/unit cell	
	Total	As Pc	C	N			Pc	CuPc
CuPcY-1(e)	1.2	0.41	5.50	1.91	203	0.11	0.9	0.7
CuPcY-2(e)	0.6	0.46	4.68	1.74	573	0.22	0.5	0.8
CuY	1.2	–	–	–	678	0.27	–	–

[a] Degassing of sample done at 423 K and 10^{-5} mm prior to N_2 adsorption.

presented in Fig. 1. Combustion of the Pc occurs rapidly in a narrow temperature region with the DTG minimum at about 693 K for the physical mixture (Fig. 1b), while the combustion occurs more slowly, in a much broader temperature range, with the DTG minimum around 750–800 K for CuPcY-1(e) (Fig. 1a). The greater difficulty in the combustion of the organics in CuPcY-1(e) suggests that the Pc is encapsulated inside the cages, and not adsorbed on the external surface.

3.2. N_2 adsorption studies

The micropore volumes and S_{BET} values of CuPcY-1(e), CuPcY-2(e), and CuY, are presented in Table 1. The surface area is found to decrease on encapsulation. The disproportionately large decrease in the pore volume and surface areas (from 0.22 to 0.11 ml/g, and from 573 to 203 m^2/g, respectively) with a small increase in total Pc content (from 1.3 to 1.6) is probably related to encapsulation occurring mainly in the more accessible cages at the periphery of the crystallites, and not uniformly throughout the bulk of the crystallites. As the α-cages of zeolite Y are interlinked, the blockage of one cage at the periphery can reduce the accessibility to many more cages in the interior. A large decrease in pore volume and S_{BET} of zeolite X on encapsulation by CuPc has been reported already by earlier workers [16].

3.3. FT-IR spectra

Representative FT-IR spectra of CuPc, CuPcY-2(e), and CuPcY(m), are shown in Fig. 2. The bands at 1462 and 1087 cm^{-1} are

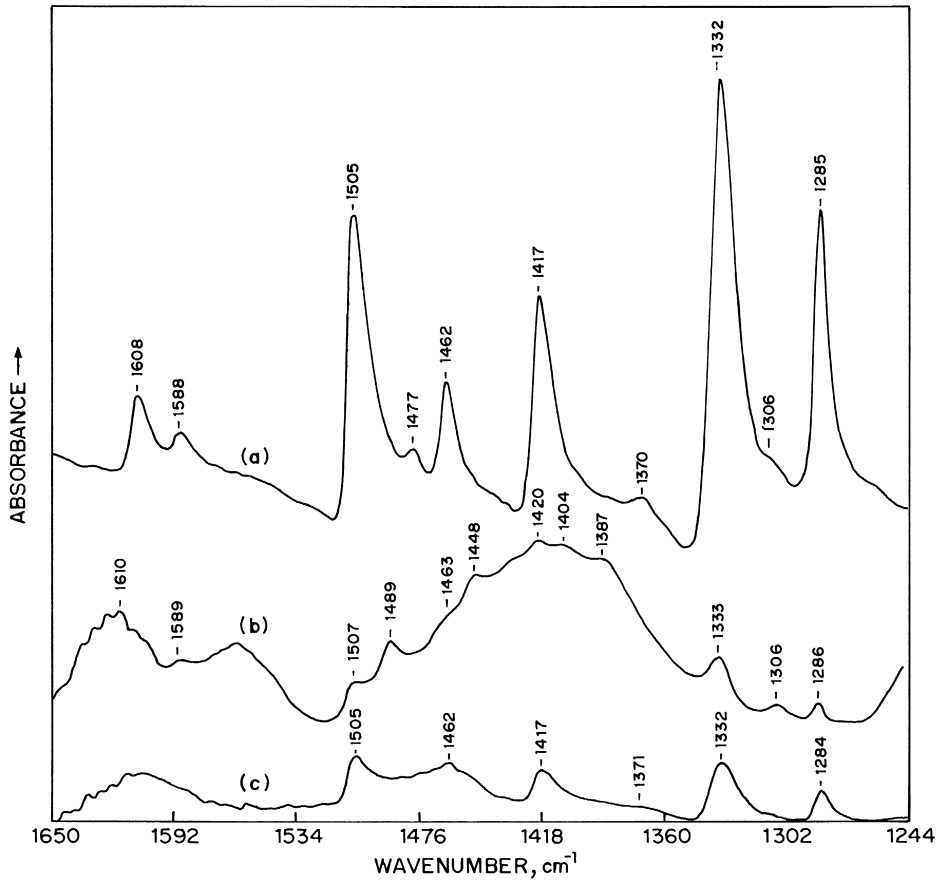

Fig. 2. FT-IR spectra of (a) ''neat'' CuPc as a KBr pellet, (b) CuPcY-1(e), and (c) CuPcY(m) as thin films.

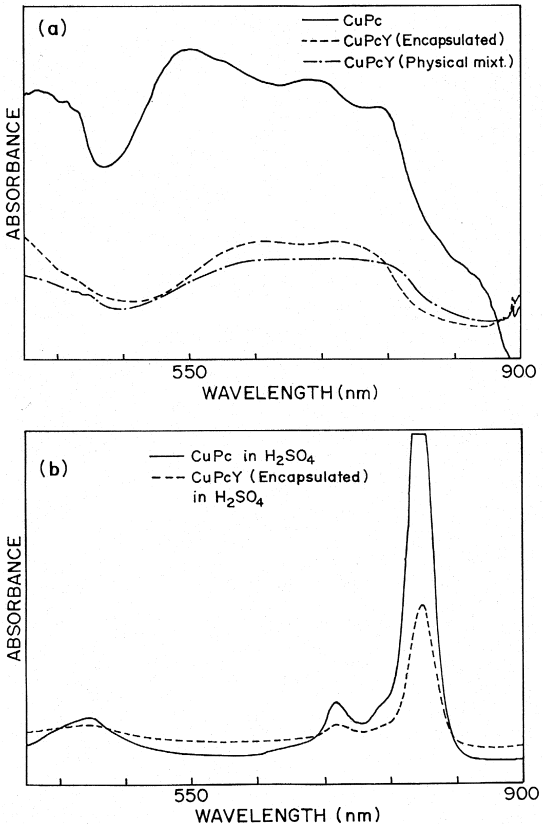

Fig. 3. (a) Diffuse reflectance UV–Vis spectra of ''neat'' CuPc, CuPcY-2(e) and CuPcY(m) and (b) absorption spectra for ''neat'' CuPc and CuPcY-2(e) in H_2SO_4.

attributed to the stretching modes of C═N and C–N, respectively. Those at 1118 and 1065 cm^{-1} correspond to the bending modes of C–H. The spectra give clear evidence for the formation of macrocyclic copper(II) phthalocyanine molecules in the supercages of NaY [17–20]. While there is no notable shift in peak positions of the physical mixture CuPcY(m) compared to the ''neat'' CuPc, the encapsulated material CuPcY-2(e) exhibits considerable shift of the peaks at 1477 and 1370 cm^{-1} and reveals additional peaks at 1404, 1387, and 1306 cm^{-1}. The band at 1417 cm^{-1} due to ν(C═C) for ''neat'' CuPc shifts to 1448 cm^{-1} for CuPcY-2(e). This disparity between CuPcY(m) and CuPcY-2(e) could be accounted for by a change in molecular symmetry of CuPc in the encapsulated state. These results are in concurrence with the UV–Vis and EPR spectral data of these materials (vide infra).

3.4. UV–Vis spectra

Fig. 3 shows typical UV–Vis spectra for CuPc, CuPcY-2(e), and CuPcY(m) in the solid state, and that of CuPc and CuPc-2(e) dissolved in concentrated sulfuric acid. Phthalocyanine exhibits two characteristic ligand based $\pi-\pi^*$ transitions referred to as the Q bands in the visible and near IR regions. For symmetry lower than D_{4h}, these bands further split and show vibrational overtones Q(0,1) and Q(1,1) as shoulders or resolved bands [21,22]. The materials under consideration exhibit these bands in the region 550–760 nm (Table 2). It is obvious from Fig.3 and Table 2 that the Q-bands for CuPcY-2(e) and CuPcY(m) have red shifted, the shift being more pronounced in the case of CuPcY-2(e) (e.g., the band at 545 nm for the complex is shifted to 581 nm for the encapsulated sample, and to 574 nm for the physical mixture) [23]. The red shifts and changes in the relative intensities of the Q bands are probably due to changes in the molecular structure from planar to puckered geometry and isolation of the molecules. However, the spectrum in concentrated sulfuric acid is almost similar for both ''neat'' CuPc and CuPcY-2(e) confirming the presence of CuPc in the latter sample. In addition to the Q-bands, the Soret band appears around 430 nm. The latter is broad due to overlap of band attributable to $n-\pi^*$ transition [22].

Table 2
Electronic spectral data for CuPc, CuPcY-2(e), and CuPcY(m)

Sample	Soret band (nm)	Q-bands (nm)
CuPc (neat)	429	545, 588, 686, 755
CuPcY-2(e)	429	581, 595, 706, 746
CuPcY(m)	429	574, 592, 699, 755
CuPc in H_2SO_4	443	702, 795
CuPcY-2(e) in H_2SO_4	443	702, 795

3.5. EPR spectra

EPR spectra (Figs. 4 and 5) give unequivocal evidence for the encapsulation of CuPc in the supercages of zeolite Y. The spectra for solid samples of CuY show the presence of two types of Cu(II) species at 298 K. Species I is characterized by a rhombic g tensor with $g_x = 2.083$, $g_y = 2.095$, and $g_z = 2.376$. Hyperfine features due to copper could be resolved in the parallel (g_z) region, while the values in the perpendicular (g_x, g_y) region were obtained by spectral simulations ($A_x = A_y = 10$ G and $A_z = 119$ G). Species II exhibits an isotropic signal at $g_{iso} = 2.166$. A typical spectrum for CuY (1.2 wt.%) is depicted in Fig. 4a. Upon lowering the temperature to 77 K, the spectrum corresponds to that of three inequivalent species (Fig. 5a). While the g values of species I are marginally affected, species II, which shows an isotropic signal at 298 K, transforms into two species (II′

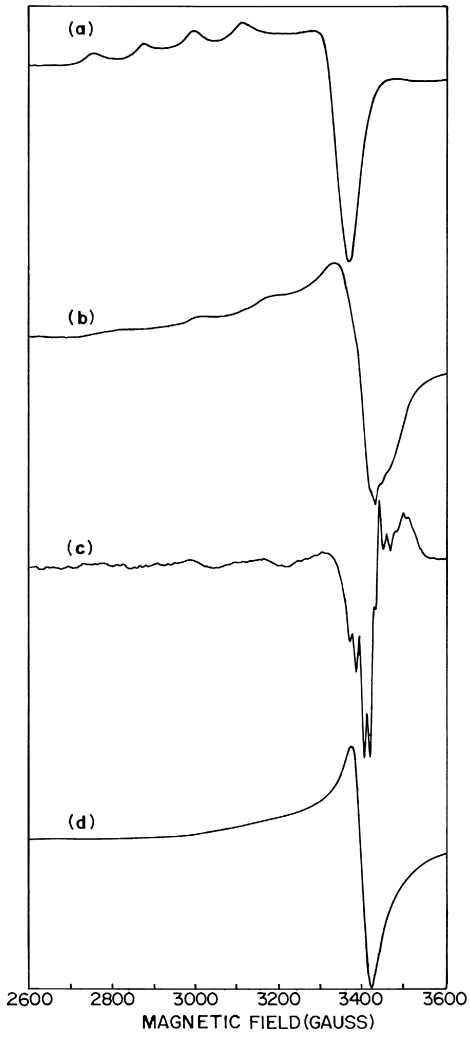

Fig. 4. X-band EPR spectra at 298 K for the powder samples of (a) 1.2 wt.% CuY, (b) CuPcY-1(e), (c) same as (b) but in 2nd derivative mode showing resolution of superhyperfine features in perpendicular region due to four equivalent nitrogens of Pc moiety, and (d) CuPcY(m).

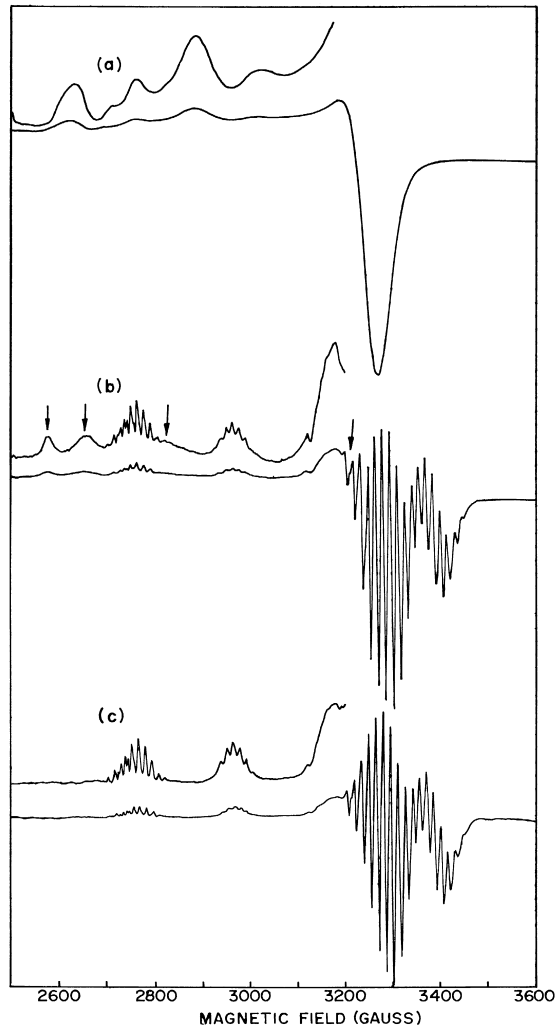

Fig. 5. X-band EPR spectra at 77 K for (a) 1.2 wt.% CuY, showing signals corresponding to three inequivalent sites, (b) and (c) frozen H_2SO_4 solutions of CuPcY-1(e) and ''neat'' CuPc; besides the CuPc signals, uncomplexed Cu (II) ions (marked by arrows) are also noticed in spectrum (b).

and II″) at 77 K characterized by axial g and A (Cu) tensors. The EPR parameters listed in Table 3 agree with those reported by others [24,25]. Species I is attributed to Cu(II) ions in the sodalite cages and II to the sites near the hexagonal prism and in the supercages (α-cages). The latter species undergo a dynamic Jahn–Teller effect at ambient temperatures and becomes static below 265 K.

The spectrum for ''neat'' CuPc reveals near neighbouring interactions and shows dipolar broadened EPR signals at $g_{\|} = 2.133$ and $g_{\perp} = 2.045$. However, when CuPc moieties are isolated (as is the case in doped systems and frozen solutions), one would observe $2nI + 1$ (nine) superhyperfine features due to four equivalent nitrogens of the isoindole groups, apart from the four hyperfine features due to copper [26,27]. ^{14}N has a nuclear spin (I) of 1, while ^{63}Cu and ^{65}Cu have nuclear spins of $3/2$. Indeed, such superhyperfine features are seen in the perpendicular region of CuPcY-1(e) (Fig. 4b and the 2nd derivative spectrum Fig. 4c shown for clarity). A closer look at the spectrum shows additional signals indicated by arrows corresponding to the Cu(II) ion in the sodalite cage along with the signals due to CuPc. The spectrum for the physical mixture, CuPcY(m), is shown in Fig. 4d. Although the signals are narrowed due to dilution, the Hamiltonian parameters are different and hyperfine, and superhyperfine features could not be resolved unlike that of CuPcY-1(e). A frozen H_2SO_4 solution of CuPcY-1(e) at 77 K (Fig. 5b) showed well-resolved spectra with a rich number of hyperfine and superhyperfine signals. A comparison of the spectrum with that of ''neat'' CuPc in H_2SO_4 (Fig. 5c) and the nine superhyperfine features (in both parallel and perpendicular regions), clearly indicate the formation of CuPc and confirms the coordination of four nitrogens of the macrocyclic Pc moiety with Cu(II). Interestingly, hyperfine features due to ^{63}Cu and ^{65}Cu are also resolved. Further, the absence of signals due to sites II′ and II″ indicate that only the Cu(II) ions in the supercages or those near the hexagonal prisms inside the supercages undergo complexation, while the ions in the sodalite cages are inaccessible. The g values (Table 3) with $g_{\|} > g_{\perp}$ suggest that the unpaired electron of ''neat'' and encapsulated CuPc occupies a ''formal'' $3d_{x^2-y^2}$ orbital of the metal ion. Also, the deviation of g and A(Cu) from that of CuPc diluted in ZnPc and H_2Pc [22,23], and the frozen H_2SO_4 spectra in this work, suggests that the confinement of CuPc in zeolite supercages has a significant effect on the molecular geometry of Pc. The larger $g_{\|}$ value for CuPcY-1(e) corresponds to that of a pentacoordinated geometry for copper with the Pc moiety being puckered in the supercages while it is planer in ''neat'' and frozen solutions.

Table 3
EPR spin Hamiltonian parameters for CuY, CuPcY-1(e) and CuPcY(m)[a]

Sample	Temperature (K)	Species	$g_{\|}$ (or g_z)	$g_{\perp}$ (or g_x, g_y)	$A_{\|}$ (Cu) (G)	$A_{\perp}$ (Cu) (G)	$A_{\|}$ (N) (G)	$A_{\perp}$ (N)
CuY	298	I	2.376	2.083	119.0	10.0	–	–
				2.095		10.0		
		II	2.166	2.166	NR	NR	–	–
	77	I	2.384	2.086	127.9	NR	–	–
		II′	2.415	2.086	119.4	NR	–	–
		II″	2.280	2.077	137.5	NR	–	–
CuPc	298		2.133	2.045	NR	NR	NR	NR
CuPcY-1(e)	298		2.246	2.056	189.5	14.2	NR	NR
CuPcY(m)	298		2.205	2.051	NR	NR	NR	NR
CuPc in H_2SO_4	77		2.200	2.062	196.5 (207.0)	11.0 (11.0)	13.2	16.0
CuPcY-1(e) in H_2SO_4	77		2.200	2.062	196.5 (207.0)	11.0 (11.0)	13.2	16.0

[a] NR = not resolved.

Table 4
Product distribution in styrene oxidation
Conditions: styrene, 4.8 mmol; acetonitrile, 5 g, tertiary butylhydroperoxide, 4.8 mmol, Aldrich; catalyst, 0.05 g, except where noted; temperature, 333 K.

Catalyst	Cu[a] (exchange) (wt.%)	Cu as CuPc (wt.%)	Conversion (wt.%)	TON[b] (h^{-1})	Product distribution[c]			
					–CHO	EPO	$-CH_2CHO$	Others
CuPcY-1(e)	0.79	0.41	94.2	50.3*	43.5	39.1	13.7	3.8
CuPcY-2(e)	0.14	0.46	95.2	51.2*	53.0	23.8	12.6	10.5
CuPcY-1(e)-Ca	0.09	0.41	63.4	38.7*	52.4	34.3	9.0	4.2
CuPc (4 mg)	–	–	29.3	8.4*	50.1	40.6	7.8	1.7
CuY	1.2	–	20.9	4.5†	64.2	29.5	6.2	0.2

[a] Cu in exchange sites (uncomplexed with Pc).
[b] Moles of styrene converted per mole of active component per hour.
[c] –CHO = benzaldehyde, EPO = styrene epoxide, $-CH_2CHO$ = phenylacetadehyde.
* based on CuPc.
† based on Cu ions in exchange positions.

3.6. Catalytic activity

The results of the catalytic activity studies carried out in the epoxidation of styrene over the encapsulated and neat CuPc complexes and a parent CuY sample are presented in Table 4. It is noticed that the encapsulated complexes are more active than the neat complex and the parent CuY. For example, CuPcY-1(e) gives a conversion of 94.2%, whereas, the neat complex (4 mg, more than double the 1.8 mg of CuPc present in 0.05 g of CuPcY-1(e) used in the reaction) gives a conversion of only 29.3%. Again, CuY (1.2%) gives a conversion of 20.9%. Analyzing the above data, in terms of TON (moles converted per mole of CuPc or Cu ions per hour) we get a value of 8.4 for CuPc and 4.5 for CuY. After correcting for the anticipated conversion, due to the exchanged (unreacted) Cu present in CuPcY-1(e), one gets a TON of 50.3 for the encapsulated Pc molecules. The TON for CuPc in CuPcY-2(e) and CuPcY-1(e)-Ca are 51.2 and 38.7, respectively. Though the values for CuPcY-1(e) and CuPcY-2(e) are similar (50.3 and 51.2), the TON for CuPc-1(e) after Ca-exchanging is slightly lower (38.7). The reasons for the observed effect of Ca on activity are not clear. The above results indicate that activation of the CuPc molecules takes place when they are encapsulated inside the cages of Y. A similar enhancement in the activity of CuPc on encapsulation in zeolite Y has been reported by Ernst et al. [28] in the case of ethylbenzene oxidation. The higher activities of the complexes noticed on encapsulation may be a result of the distortion of the molecules (revealed by spectroscopic studies) and the consequent ease of redox transformations of Cu ions.

4. Conclusions

Spectroscopic studies, as well as chemical and thermal analyses, present clear evidence for the formation and encapsulation of CuPc in the supercages (α-cages) of zeolite Y. The presence of additional IR peaks, red shift in Q-bands, and changes in g and A(Cu) values, correspond to distortion in the square planar geometry or puckering of the phthalocyanine moiety in the encapsulated state. EPR studies also reveal that though exchanged Cu(II) ions are present in both the supercages (α-cages) and sodalite cages (β-cages) in CuY, only those present in the larger α-cages react to form the complexes. Even though both the Cu ions and CuPc are catalyticaly active in the epoxidation of styrene, the encapsulated complexes are many-fold more

active. The enhancement of the activity of the CuPc inside the cages could be a result of the distortion of the CuPc molecules.

Acknowledgements

Sindhu Seelan thanks C.S.I.R., New Delhi for the award of a Senior Research Fellowship. The authors thank Dr. S.G. Hegde and Mrs. N.E. Jacob for their help.

References

[1] K.J. Balkus Jr., A.G. Gabrielov, J. Inclusion Phenom. Mol. Recognit. Chem. 21 (1995) 159.
[2] R. Parton, D. De Vos, P.A. Jacobs, in: E.G. Derouane, F. Lemos, C. Naccache, F.R. Riberio (Eds.), Proceedings of NATO Advanced Study Institute on Zeolite, Microporous Solids: Synthesis, Structure and Reactivity 555 Kluwer, Dodrecht, 1992, p. 578.
[3] D.E. De Vos, F. Thibault-Starzyk, P.P. Knops-Gerrits, R.F. Parton, P.A. Jacobs, Macromol. Symp. 80 (1994) 157.
[4] N. Herron, Inorg. Chem. 25 (1986) 4714.
[5] C.R. Jacob, S.P. Varkey, P. Ratnasamy, Appl. Catal., A 168 (1998) 353.
[6] B.T. Holland, C. Walkup, A. Stein, J. Phys. Chem. B 102 (1998) 4301.
[7] R. Raja, P. Ratnasamy, Stud. Surf. Sci. Catal. 101 (1996) 181.
[8] E. Armengol, A. Corma, V. Fornes, H. Garcia, J. Primo, Appl. Catal. 181 (1999) 305.
[9] V.Yu. Zakharov, O.M. Zakharova, B.V. Romanovsky, R.E. Mardelishvili, React. Kinet. Catal. Lett. 6 (1977) 133.
[10] G. Meyer, D. Wöhrle, M. Mohl, G. Schulz-Ekloff, Zeolites 4 (1984) 30.
[11] N. Herron, G.D. Stucky, C.B. Tolman, J. Chem. Soc., Chem. Commun. (1986) 1521.
[12] M. Ichikawa, T. Kimura, A. Fukuoka, Stud. Surf. Sci. Catal. 60 (1991) 335.
[13] V.Yu. Zakharov, B.V. Romanovsky, Vestn. Mosk. Univ., Khim. 18 (1977) 142.
[14] B.V. Romanovsky, in: Y. Yermakov, V. Likholobov (Eds.), Homogeneous and Heterogeneous Catalysis, VNU Science, Utrecht, 1986, p. 343.
[15] K.J. Balkus Jr., J.P. Ferraris, J. Phys. Chem. 94 (1990) 8019.
[16] R. Raja, P. Ratnasamy, J. Catal. 170 (1997) 244.
[17] M. Fukui, N. Katayama, Y. Ozaki, T. Araki, K. Iriyama, Chem. Phys. Lett. 177 (1991) 247.
[18] R. Aroca, Z.Q. Zeng, J. Mink, J. Phys. Chem. Solids 51 (1990) 135.
[19] R. Parton, PhD Thesis, K.U. Leuven, Belgium, May 1993.
[20] J. Dowdy, J.J. Hoagland, K.W. Hipps, J. Phys. Chem. 95 (1991) 3751.
[21] A.B.P. Lever, Adv. Inorg. Chem. Radiochem. 7 (1965) 27.
[22] K.J. Balkus Jr., M. Eissa, R. Lavado, Stud. Surf. Sci. Catal. 94 (1995) 713.
[23] K.J. Balkus Jr., A.G. Gabrielov, S.L. Bell, F. Bedioui, L. Roue, L. Davynck, Inorg. Chem. 33 (1994) 67–72.
[24] R.G. Herman, D.R. Flentge, J. Phys. Chem. 82 (1978) 720.
[25] C. Naccache, Y.B. Taarit, Chem. Phys. Lett. 11 (1971) 11.
[26] C.M. Guzy, J.B. Raynor, M.C.R. Symons, J. Chem. Soc. (1969) 2299.
[27] S.E. Harrison, J.M. Assour, J. Chem. Phys. 40 (1964) 365.
[28] S. Ernst, Y. Traa, U. Deeg, Stud. Surf. Sci.Catal. 84 (1994) 925.